Journal of Electrostatics, 25 (1990) 265–275
Elsevier

Fast computer simulation of open-air electrostatic spray painting

G.M.H. Meesters, C.A.P. Zevenhoven, J.F.J. Brons and P.J.T. Verheijen*

Department of Chemical Engineering, Delft University of Technology, P.O. Box 5045, 2600 GA Delft, The Netherlands

(Received November 23, 1989; accepted in revised form August 25, 1990)

Summary

A numerical computer simulation has been developed for the electrostatic spray paint process. The theoretical model describes the path of a cloud of charged drops. It takes into account the drop size, temperature, density, viscosity of paint and air, charge of the drops, potential of the sprayer head, the use of air assistance, air-paint ratio, paint flow, wind and turbulence and the distance towards the object. Especially the influence of the wind and wind turbulence on the spraying process was investigated. With increasing crosswind a higher charge, larger drops or air-assisted spraying will keep the efficiency high. Too much charge on the drops will cause the cloud to expand too much. Painting in the open air with a mild wind is possible using the electrostatic spray paint process.

1. Introduction

Electrostatic spray painting is a well known method in the car industry, whereby chassis are efficiently covered with a paint coating. The question has been raised whether electrostatic painting could also be done in open air, where wind and turbulence play a role. In this process the paint is sprayed by a gun, where the droplets are given an electric charge. At the same time the gun serves as a source of high voltage. In this field the droplets are driven towards an electrically earthed object. Previously Anestos [1] and Hakberg et al. [2] reported a theoretical model predicting the electric field distribution during air-atomized electrostatic spray painting, but they do not account for open-air conditions. Ang and Lloyd [3] calculated charged particle trajectories in a similar system neglecting the effect of space charge.

The purpose of the present simulation was to evaluate the whole process, and in particular to determine the influence of wind and turbulence on this method of painting. Equipment parameters variable in the simulation are: temperature, particle size, density and viscosity, charge on the droplets, poten-

*To whom correspondence should be addressed.

tial difference between sprayer and object, size of spray head, the use of air assistance, air to paint ratio, paint flow, wind and distance.

The forces acting on the particle are the electrostatic force, the drag force, the wind forces and the gravitational force, which are all included in the force balance for a particle. A fourth-order Runge–Kutta method with adaptive step size control is then implemented to follow the trajectory of the particles.

2. Wind and turbulence

The intensity and the fluctuating character of air flows have a great impact on the motion of a cloud of small droplets. Theoretically, this is introduced into the force balance through the drag force. In order to account for its statistical character, wind is regarded as a mixture of turbulent eddies, the rotating character of which can be quantified by an energy spectrum $E(\omega)$ for an eddy with angular frequency ω. If the wind turbulence is assumed to be purely the result of mechanical effects, i.e. disregarding the effects of temperature gradients and stratification, generalised relations describing atmospheric turbulence are available [4]:

$$E(\omega)=\frac{nv_0^2H/|\boldsymbol{w}_o|}{(1+mH\omega/|\boldsymbol{w}_0|)^{5/3}} \tag{1}$$

with v_0=friction velocity, H=vertical height above the ground, $|\boldsymbol{w}_0|$=time-averaged wind amplitude and n and m are constants.

The coefficients n and m are equal to: for x' (wind direction) $n=105$, $m=5.25$; for y' (horizontal, perpendicular to x') $n=17.5$, $m=1.51$; for z (vertical) $n=2.0$, $m=0.84$. In v_0 the effects of the earth surface and objects nearby are collected in a macroscopic approach. This velocity is given by

$$v_0=\frac{0.4|\boldsymbol{w}_0|}{\ln(H/h_0)} \tag{2}$$

where h_0 is a roughness height which is generally in the order of the object size (h_0=0.1–1 m [4]). The energy spectra $E(\omega)$ are related to autocorrelation functions $R(\tau)$ for the wind velocity fluctuations for each velocity component through Fourier transformation:

$$R(\tau)=\overline{w'(t)w'(t+\tau)}=\int_0^\infty E(\omega)\cos(\omega\tau)\,\mathrm{d}\omega \tag{3}$$

which means that the average value for one component of the velocity fluctuation $w'(t+\tau)$ for a time step τ can be evaluated from $w'(t)$:

$$\overline{w'(t+\tau)}=\frac{R(\tau)}{R(0)}w'(t) \tag{4}$$

Equations (1) and (3) lead to

$$R(\tau)=1.5\frac{nv_0^2}{m}\exp\left[1-3\left(\frac{|\boldsymbol{w}_0|\tau}{Hm}\right)^2\right] \tag{5}$$

for small values of τ. Equations (4) and (5) describe the decay of a velocity fluctuation that was present at $\tau=0$. On the other hand, the new fluctuations w' originating in the period τ are of a stochastic nature of which the variance is presented by

$$\mathrm{Var}(w'(t+\tau))=R(0)-R(\tau) \tag{6}$$

i.e. directly proportional to the decay of the autocorrelation functions $R(\tau)$. Using this approach the wind velocity fluctuations can be described as a (normal) distribution function which follows from the autocorrelation function $R(\tau)$, while the velocity itself may be written as the sum of a time averaged mean value and a time dependent fluctuation: $\boldsymbol{w}(t)=\boldsymbol{w}_0+\boldsymbol{w}'(t)$. Given this, the procedure for the calculation of a component of the instantaneous wind velocity is written as

$$w(t+\tau)=w_0+w'(t)\frac{R(\tau)}{R(0)}+k\sqrt{R(0)-R(\tau)} \tag{7}$$

where k is a proportionality constant derived from a standard normal distribution, generated at each time step in the calculation. The wind velocity vector $\boldsymbol{w}$ thus obtained as a function of time is inserted in the force balance described in the following section.

3. Model equations

The total force acting on a droplet is composed of the electric field force, the drag force (interactions with the air), and the gravitational force; in vectorial form [5]:

$$m_p\boldsymbol{a}=q\boldsymbol{E}+\boldsymbol{F}_D+m_p\boldsymbol{g} \tag{8}$$

the first term, $q\boldsymbol{E}$, depends primarily on the electric charge on the droplet. The charge is calculated by Rayleigh's equation for charged liquid droplets [6]:

$$q=\phi 4\pi\sqrt{0.5\sigma\epsilon_0 d_p^3} \tag{9}$$

The fraction ϕ depends on the charging process. The equation is a result of a balance between the outward electrostatic pressure (due to the charge) and the binding surface tension pressure. Any infinitesimal increase in charge above this level (when $\phi=1$) results in disruption of the drop into stable charged fragments. Several papers [7–9] report on particle charging using electrostatic atomization, finding a value for ϕ close to 0.5. For corona charging the Pauthenier limit is valid implying a far smaller value for ϕ (0.01–0.15 [10]).

The best way to describe the electric field is to create a grid in space and use

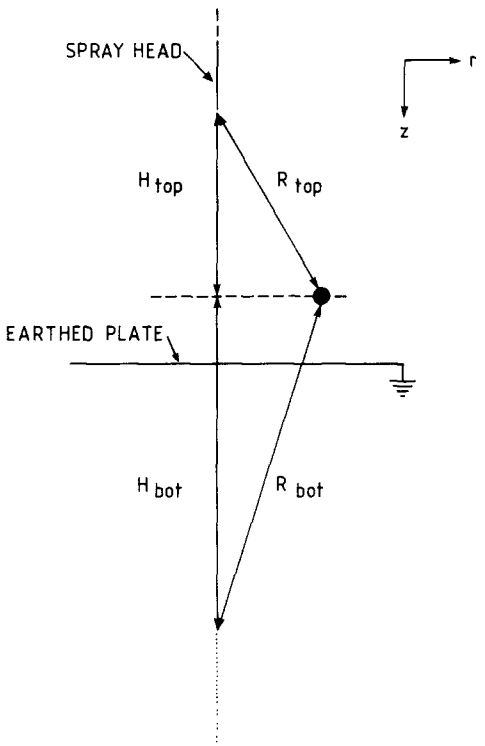

Fig. 1. Configuration of the electric field between spray head and earthed plate.

the Poisson equation accounting for space charge [2]. In each grid point the field can be calculated. To facilitate fast simulations an approximation was used. The electric field $\boldsymbol{E}$ is given by that of a semi-infinite charged line to an earthed plate (Fig. 1) from which follows [7, 11]

$$E_z = -\Gamma\left(\frac{1}{R_{\text{top}}} + \frac{1}{R_{\text{bot}}}\right) \tag{10}$$

$$E_r = \Gamma\left(\frac{H_{\text{top}}}{R_{\text{top}}} + \frac{H_{\text{bot}}}{R_{\text{bot}}}\right)\Big/ r \tag{11}$$

Γ is calculated such that the potential at the starting point equals that of the spray head.

The average charge density is calculated from the paint flow, charge on the droplets and the cross-section of the flow. Normally this is a correction to the main field, except when droplets are slowed down yielding an increase in concentration.

The second term in equation (8), the drag force $\boldsymbol{F}_{\text{D}}$ is, for a single particle, calculated by:

$$\boldsymbol{F}_D = -\tfrac{1}{2} C_D \rho_f |\boldsymbol{v}_r| \boldsymbol{v}_r \tfrac{1}{4}\pi d_p^2 \tag{12}$$

where $\boldsymbol{v}_r$ is the relative velocity of the particle with respect to the air. C_D differs with the flow regime [5]:

$$\mathrm{Re}_p < 0.1 \qquad C_D = 24/\mathrm{Re}_p \tag{13}$$

$$0.1 \leqslant \mathrm{Re}_p < 1000 \quad C_D = 24/\mathrm{Re}_p (1 + 0.14 \mathrm{Re}_p^{0.7}) \tag{14}$$

The drag resistance experienced by droplets when in a dense cloud or swarm is reduced by the wake of the surrounding droplets. This reduces the drag coefficient [12] with respect to the above mentioned to

$$C_{D,\mathrm{swarm}} = C_D (1 - \psi)^n \tag{15}$$

where ψ equals the fraction of the volume that is occupied by the droplets in the swarm. Depending on the single-particle stationary sedimentation velocity the constant n is related to the stationary Reynolds number, leading to a value between 2.39 and 4.65 [12].

Hakberg et al. [2] used Stokes law in their force balance, thus $C_D = 24/\mathrm{Re}_p$ (eqn. (13)), and Ang and Lloyd [3] used the full equation (14). We have made simulations with both cases and found significant differences, because near the spray head the Reynolds number is far too high, enforcing the use of the complete equations (13,14). The density of the air is calculated using the ideal gas law. The viscosity of the air and the surface tension of the liquid are calculated as being a function of temperature only [13–16].

4. Algorithm

At the beginning of the trajectory calculation the position and the velocity are known. With this, the force balance gives a resulting force, therefore a resulting acceleration, with which the velocity at the end of a timestep is calculated. This is a linearization that becomes incorrect where high acceleration occurs (e.g. near the spray head where the field is highly nonuniform), which is solved by taking very small time steps. The step size is controlled through an adaptive step size control for Runge–Kutta procedures [17].

Four drops that are ejected in different directions but with the same angle to the spray direction (up, down, left, right) are assumed to describe the cross-section of the paint-cloud completely as being the end points of the axes of an ellipse. Since their trajectories are calculated simultaneously, after each timestep the internal repulsion, the induced field and the drag force of the cloud are calculated easily. The calculations are performed until the four drops have arrived on the plate. Subsequently, the efficiency of the process is calculated as the relative surface area of the paint blot — ellipse — that overlaps with a predefined target circle.

5. Simulations

The program, ESPAINTF, has been used to simulate the spray paint process. The effects of the various parameters influencing the droplet transport were evaluated by varying each one separately and comparing them with a standard configuration. This chosen configuration, which closely resembles a practical situation, is presented in Table 1.

As calculated by the program, the trajectory of a cloud of droplets is described as follows: (a) the droplets leave the spray head with a high speed which is reduced by air drag; (b) the resulting retardation leads to an increasing concentration and space charge such that the repulsive forces start to dominate and significant divergence takes place; and (c) having diverged, the electric field takes over and leads the particles to the target surface. There are conditions, e.g. when the electric field is too small, where a cloud is completely scattered and only few particles reach the target.

The electrical parameter that plays a major role here is the charge on the particle as determined by the Rayleigh fraction. Figure 2 shows that there is an optimum for this fraction which is explained by the two competing processes: divergence due to the space charge and convergence towards the target by the electric field.

The geometry of the configuration is well presented by the dependence of efficiency on pistol to plate distance, as illustrated by Fig. 3. Above a certain distance, which decreases with cross wind, the electric field is not strong enough for a paint cloud to be transported to the target surface.

The drop diameter influences the particle motion through its relation to the Rayleigh charge limit for the particle, to the drag force and the inertial mass.

TABLE 1

Standard values of several adjustable parameters used.

Temperature of liquid	15 °C
Temperature of air	15 °C
Liquid density	1223 kg/m^3
Cross wind	2 m/s
Diameter of drops	50 μm
Voltage	60 kV
Rayleigh fraction	0.05
Diameter of sprayhead	0.01 m
Angle of conus	30°
Distance to target	0.3 m
Diameter of target circle	0.3 m
Initial velocity	80 m/s
Paint flow	1 l/s
Paint/air ratio	1%

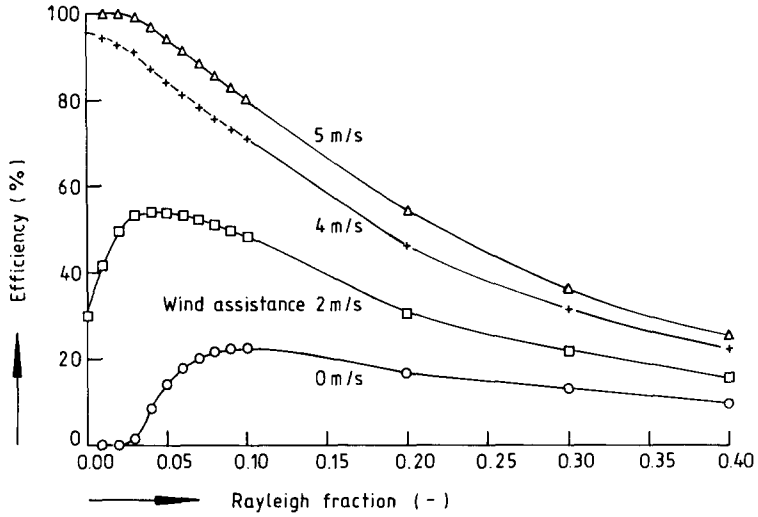

Fig. 2. The dependence of efficiency on the droplet charge at different wind conditions.

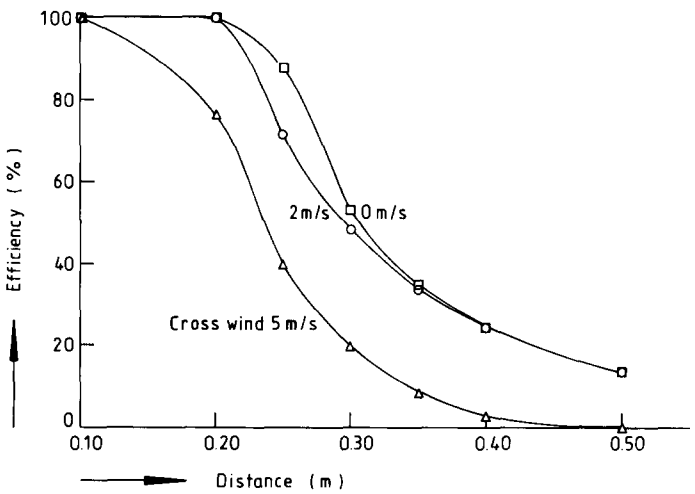

Fig. 3. Influence of the distance between the paint gun and the object on the efficiency at different magnitudes of cross wind. (Rayleigh fraction = 0.2, wind assistence = 2 m/s, other parameters see Table 1).

The total effect leads to an increase in efficiency with increasing particle size. This is quantified in Fig. 4.

Finally the presence of air movement, i.e. air assistance and/or cross wind, forms a major determining factor in the cloud movement. Figure 5 shows that efficiency rapidly drops with cross wind. Such an effect is also obvious in Figs.

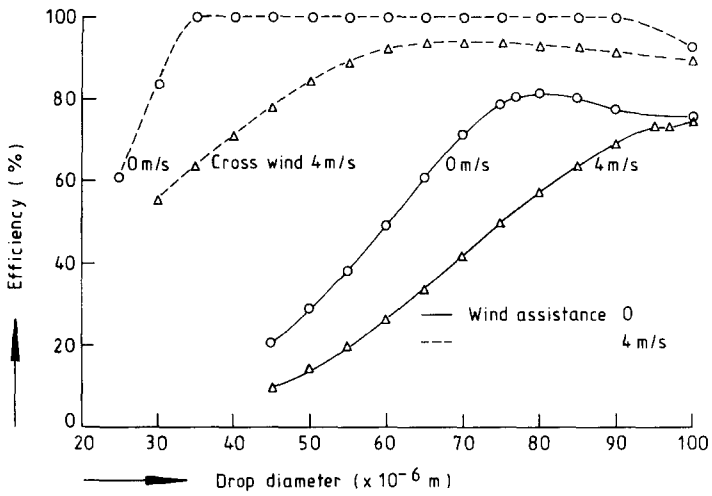

Fig. 4. Influence of the paint drop diameter on the paint efficiency with cross wind and wind assistance.

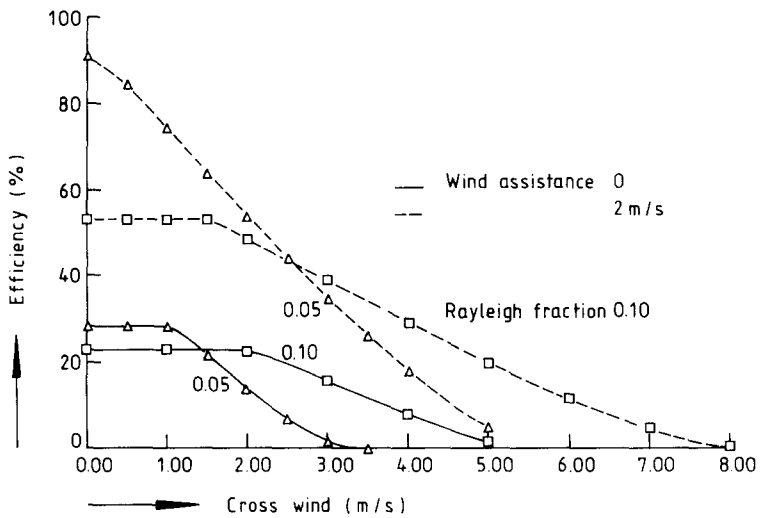

Fig. 5. The relation between efficiency and cross wind.

3 and 4. Air assistance always improves efficiency, as is obvious. However, even moderate adverse wind dramatically reduces efficiency.

The program also showed that the fluctuating component of the wind has a relatively small effect on the efficiency. For example, the standard configuration (Table 1), simulated for forty times caused a spread of 0.40% (s.d.) in an average efficiency of 13.11%.

Factors of little direct influence on the calculated efficiencies are: tempera-

ture and the physical properties of the liquid comprising the droplets. Also the emission angle from the target appeared to have little effect on the efficiency since it is the electric field that guides the droplets finally.

Difficulties in the simulations occurred for particles leaving the spray head slowly. This is a part of the electric field where the simple approximation eqns. (10) and (11) is the least valid. Also the conditions where the space charge causes a complete breakup of the cloud could not be simulated with the present formulas and the trajectory calculation was halted.

6. Discussion and conclusions

The described program provides for an interactive and user friendly method of simulating of the electrostatic spray paint process. A typical simulation takes 20 seconds on an AT personal computer.

The relatively simple method of calculation allowed this speed, but its applicability is limited by the underlying assumptions and idealization. The most apparent complication occurs sometimes when the velocity of the droplets decreases to the point where the repulsive force from the space charge exceeds the force from the externally applied electric field (e.g. with a high charge per droplet or with a low spray gun voltage). A second complication was found in describing what happens near the spray head (e.g. slightly charged particles cannot have emission angles exceeding 45°). Finally, the fringe effects of a finite target are obviously not accounted for, but this does not impose serious limitations for flat surface objects since the description of the electric field near the object is not a highly determining factor in the efficiency.

These three aspects can be better accounted for with the full Poisson equation of an electric field with space charge, especially near the spray head where the present equations have a singularity. Nonetheless, the present program has proven to be capable of simulating for a wide range of process parameters (Figs. 2–5), whereby the simulated paint cloud movement strongly resembles the shape of paint clouds observed in the actual process of electrostatic spray painting.

No account has been taken of any particle charge or size distribution. Hakberg et al. [2] measured and mentioned a size distribution in the experiments but did not state whether this was used in the simulations as well. In consequence of experiments with 10 μm particles in another laboratory (COT, Haarlem, The Netherlands), we have included the effect of a size distribution into the simulations by averaging eqns. (8) and (15) over the distribution adding the assumption that the surface charge could be considered constant. Our simulation using parameters resembling an actual experiment but with a monosize distribution led to the prediction that the particles were prevented by space charge to reach the target. The simulation with the same parameters but with a size distribution obtained from photographic observations, gave a

regular behaviour as described in the previous section. This was in agreement with the experiment. Size and charge distributions must therefore be known in order to simulate practical situations more quantitatively.

With respect to conclusions to be drawn for outdoor spray painting it is clear that spray painting using air assistance will increase the efficiency. There obviously is an optimum for the charge per particle, depending on the other parameters.

Figure 4 shows that the distance between the sprayer head and object is very important. A variation of a few centimeters can cause a rapid change in efficiency, visualized by the slope of the curves.

Painting in open air under mild circumstances is possible, especially when air assisted sprayers are used. Because of the electrostatic force many droplets which would (without a charge) have been blown away are now still attracted by the object because of their charge, thereby decreasing the loss of paint. Turbulent fluctuations do not influence the efficiency of the process dramatically.

List of symbols

$\boldsymbol{a}$	acceleration (vector) [m/s^2]
C_D	Drag coefficient [–]
d_p	drop diameter [m]
$\boldsymbol{E}$	electric field strength (vector) [V/m]
$E(\omega)$	energy spectrum [J]
$\boldsymbol{F}$	force (vector) [N]
$\boldsymbol{F}_D$	drag force [N]
g	gravitational acceleration [m/s^2]
h_0	roughness height [m]
H	vertical height above the ground [m]
m_p	mass of particle [kg]
m, n	constants [–]
q	charge [C]
r	radial distance $\sqrt{x^2+y^2}$ [m]
R	distance [m]
$R(\tau)$	autocorrelation function [J]
Re_p	Reynolds number [–]
$\boldsymbol{v}_r$	relative velocity with respect to air [m/s]
v_0	friction velocity [m/s]
$\boldsymbol{w}$	wind (vector) [m/s]
$\boldsymbol{w}_0$	constant part of the wind vector [m/s]
$\boldsymbol{w}'$	fluctuating part of the wind vector [m/s]
x,y,z	coordinate system [m]
x',y'	coordinates for wind vector [m]

Γ coefficient [V]
ϵ_0 permittivity of free space [F/m]
ρ density [kg/m^3]
σ surface tension [N/m]
τ timestep [s]
ϕ fraction of maximum charge [–]
ψ volume concentration [–]
ω angular frequency [1/s]

Acknowledgements

This project has been financially supported by the Ministry of Social Affairs and the COT, Center for Research and Technical Advice, Haarlem, The Netherlands. We are grateful to Capt. L. Brink for his encouragement.

References

1 T.C. Anestos, IEEE Trans. Ind. Appl., 1 (1986) 70.
2 B. Hakberg, S. Lundqvist, B. Carlsson and T. Hogberg, J. Electrostat., 14 (1983) 255.
3 M.L. Ang and P.J. Lloyd, Int. J. Multiphase Flow, 13 (1987) 823.
4 H.A. Panofsky and J.A. Dutton, Atmospheric Turbulence, Wiley and Sons, 1984.
5 H. Schubert, E. Heidenreich, F. Liepe and T. Neesse, Mechanische Verfahrenstechnik, VEB Deutscher Verlag für Grundstoffindustrie, 2nd ed., 1985.
6 Rayleigh, Lord, Proc. R. Soc. London, 24 (1879) 71.
7 A.R. Jones and K.C. Thong, J. Phys. D, Appl. Phys., 4 (1971) 1159.
8 S.B. Sample and R. Bollini, J. Colloid Interface Sci., 11 (2) (1972) 185.
9 R.J. Pfeifer and C.D. Hendricks, Phys. Fluids, 10 (1967) 2149.
10 J.A. Cross, Electrostatics: Principles, Problems and Applications, Hilger, New York, 1984.
11 A. Gay and G.B. Matthew, A Treatise on Besselfunctions and their Applications to Physics, Macmillan, London, 1922.
12 J.F. Richardson and W.N. Zaki, Trans. Inst. Chem. Eng., 32 (1954) 35.
13 J.H. Arnold, J. Chem. Phys., 1 (1933) 170.
14 W.R. Gambill, Chem. Eng., (1955) 207.
15 J.H. Perry, Chemical Engineers Handbook, McGraw-Hill, New York, 6th edn., 1984.
16 S. Lövgren, Svensk Kem. Tidskr., 53 (1941) 359.
17 W.H. Press, B.P. Flannery, S.A. Teukolsky and W.T. Vetterling, Numerical Recipes, Cambridge University Press, 1986, p. 574.